Int. J. Heat Mass Transfer. Vol. 24, No. 8, pp. 1295–1303, 1981.
Printed in Great Britain

0017-9310/81/081295-09 $02.00/0

COMPUTER-EXTENDED SERIES: NATURAL CONVECTION IN A LONG HORIZONTAL PIPE WITH DIFFERENT END TEMPERATURES

TSAN-HSING SHIH†
Department of Modern Mechanics, Chinese University of Science and Technology, Peoples' Republic of China

(*Received* 27 *August* 1980 *and in revised form* 15 *December* 1980)

Abstract—For the velocity and temperature distributions in the middle portion of a long horizontal pipe with adiabatic walls and differentially heated ends, the three-term expansion of Bejan and Tien is extended to 47 terms in the Rayleigh number. We examine the series for Nusselt number, and extend its utility by analyzing its singularities. We also estimate the effect of the ends by matching the first-order core solution with an integral solution for the flow and temperature in the end region.

NOMENCLATURE

C,	wall thermal resistance parameter, equation (7);
C_n,	coefficients, equation (21);
f_n,	coefficients, equation (26);
g,	gravitational acceleration [m s^{-2}];
g_n,	coefficients, equation (25);
K,	fluid thermal conductivity [W m^{-1} K^{-1}];
K_1, K_2,	constants of zeroth-order solution, equation (14d);
L,	pipe length [m];
Nu,	Nusselt number, equation (17);
Pr,	Prandtl number [ν/α];
P,	dimensionless pressure, equation (3c);
P^*,	pressure [N m^{-2}];
Q,	convective heat flux [W];
r,	dimensionless radial position, equation (3a);
r^*,	radial position [m];
r_0,	radius [m];
Ra,	Rayleigh number, equation (3d);
t,	wall thickness [m];
T,	dimensionless temperature, equation (3c);
T^*,	temperature [K];
T_1^*, T_2^*,	cold and warm end temperatures;
u, v, w,	dimensionless radial, circumferential, axial velocities, equation (3b);
u^*, v^*, w^*,	radial, circumferential, axial velocities [m s^{-1}];
z,	dimensionless axial position, equation (3a);
z^*,	axial positions [m].

Greek symbols

α,	fluid thermal diffusivity [m^2 s^{-1}];
β,	coefficient of volumetric thermal expansion [K^{-1}];
θ,	angular position;
ν,	kinematic viscosity [m^2 s^{-1}];
ρ,	density [kg m^{-3}];
ψ,	stream function, equation (9).

Subscripts

0,	zeroth-order approximation;
n,	nth order approximations.

1. INTRODUCTION

COMPUTER extension of perturbation series in fluid mechanics has extensively been studied in recent years [1–3]. All the work indicates that this technique is able to solve a variety of problems in fluid mechanics. In general, this technique consists of three procedures. First, form a perturbation series solution to the physical problem. A modern computer makes it possible to obtain dozens or even hundreds of terms, which contain sufficient information about the analytical structure of the solution. Second, analyze the singularities of the perturbation series solution. Finally, recast the series in order to obtain an analytical expression for the solution. In the second and third procedures there is a variety of devices to be used such as Ratio method, Neville table, Padé method and some special transformations.

This paper uses computer-extended series to deal with the velocity and temperature distribution in the middle portion of a horizontal pipe with different end temperatures, and analyzes the heat transfer through the pipe. Bejan and Tien [4] studied this problem and presented a second-order perturbation solution in Rayleigh number, Ra (based on end-to-end temperature differences) for the velocity, temperature distribution and heat transfer. They point out that their

† Present address: Department of Mechanical Engineering, Stanford University, Stanford, CA 94305, U.S.A.

solution is valid only when the Rayleigh number is very small, and for cases in which the Rayleigh number is not small, the higher-order terms beyond the second will be needed. As a matter of fact, in many real problems the Rayleigh number is quite large rather than small. Therefore, we extend their second-order solution to 47th order and obtain a 24-term Nusselt number series in Ra^2. We further improve the utility of the series by analyzing the singularities of the series with Padé and Ratio methods [5]. We obtain an analytical expression for the Nusselt number, valid in all ranges of Rayleigh numbers ($0 < Ra < \infty$). Finally, we adopt Bejan and Tien's technique to estimate the effect of the ends of the pipe on the heat transfer by matching the first-order core solution with an integral solution for the flow and temperature in the end region. We find that the effect is very strong as Ra increases.

2. EQUATIONS AND PERTURBATION SERIES

The system of coordinates, r, θ, z and velocity components, u, v, w are indicated in Fig. 1. T and P stand for fluid temperature and pressure, respectively. The steady-state governing equations are

$$\frac{u}{r}+\frac{\partial u}{\partial r}+\frac{1}{r}\frac{\partial v}{\partial \theta}+\frac{\partial w}{\partial z}=0 \tag{1}$$

$$\frac{1}{Pr}\left(u\frac{\partial u}{\partial r}+\frac{v}{r}\frac{\partial u}{\partial \theta}+w\frac{\partial u}{\partial z}-\frac{v^2}{r}\right)=-\frac{gr_0^3}{\alpha\nu}\sin\theta + Ra(\sin\theta)\,T-\frac{\partial p}{\partial r}+\nabla^2 u-\frac{u}{r^2}-\frac{2}{r^2}\frac{\partial v}{\partial \theta} \tag{2a}$$

$$\frac{1}{Pr}\left(u\frac{\partial v}{\partial r}+\frac{v}{r}\frac{\partial v}{\partial \theta}+w\frac{\partial v}{\partial z}+\frac{uv}{r}\right)=-\frac{gr_0^3}{\alpha\nu}\cos\theta + Ra(\cos\theta)\,T-\frac{1}{r}\frac{\partial p}{\partial \theta}+\nabla^2 v+\frac{2}{r^2}\frac{\partial u}{\partial \theta}-\frac{u}{r^2} \tag{2b}$$

$$\frac{1}{Pr}\left(u\frac{\partial w}{\partial r}+\frac{v}{r}\frac{\partial w}{\partial \theta}+w\frac{\partial w}{\partial z}\right)=-\frac{\partial p}{\partial z}+\nabla^2 w \tag{2c}$$

$$u\frac{\partial T}{\partial r}+\frac{v}{r}\frac{\partial T}{\partial \theta}+w\frac{\partial T}{\partial z}=\nabla^2 T. \tag{3}$$

The variables and parameter in equations (1)–(3) have been nondimensionalized as follows:

$$r=r^*/r_0,\quad z=z^*/r_0 \tag{3a}$$

$$u=u^*r_0/\alpha,\quad v=v^*r_0/\alpha,\quad w=w^*r_0/\alpha \tag{3b}$$

$$T=(T^*-T_1^*)/(T_2-T_1^*),\quad p=p^*r_0^2/(\rho\alpha\nu),\quad \alpha=k/(\rho C_p) \tag{3c}$$

$$Ra=g\beta r_0^3\,(T_2^*-T_1^*)/(\alpha\nu) \tag{3d}$$

where the quantities denoted by an asterisk represent the dimensional variables of the problem. ρ, ν and k are density, kinematic viscosity and thermal conductivity. ∇^2 is the Laplace operator in cylindrical coordinates

$$\nabla^2=\frac{\partial^2}{\partial r^2}+\frac{1}{r}\frac{\partial}{\partial r}+\frac{1}{r^2}\frac{\partial^2}{\partial \theta^2}+\frac{\partial^2}{\partial z^2}. \tag{4}$$

The Boussinesq approximation has been used in the vertical momentum equation

$$\rho=\rho_1\,[1-\beta(T^*-T_1^*)] \tag{5}$$

where β is the coefficient of volumetric thermal expansion. The boundary conditions are

$$u=v=w=0 \quad \text{at } r=1 \tag{6a}$$

$$\frac{\partial^2 T}{\partial z^2}+\frac{1}{r^2}\frac{\partial^2 T}{\partial \theta^2}=C\frac{\partial T}{\partial r} \quad \text{at } r=1. \tag{6b}$$

Where C is a measure of circumferential thermal resistance of the wall relative to that of the fluid

$$C=\frac{kr_0}{k_w t}. \tag{7}$$

If $C\to\infty$ the wall is adiabatic and if $C\to 0$ the wall is isothermal. If we assume that in the middle portion of the pipe – the core region – the flow can be considered as fully developed, i.e.

$$\frac{\partial u}{\partial z}=\frac{\partial v}{\partial z}=\frac{\partial w}{\partial z}=0. \tag{8}$$

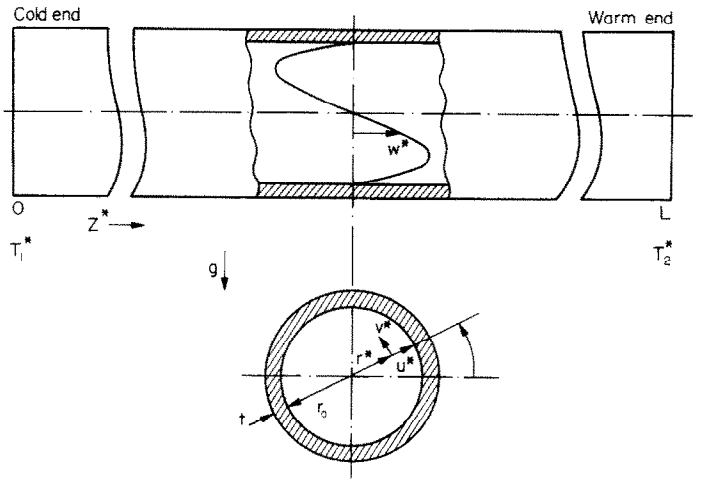

FIG. 1. Natural counterflow in a long horizontal pipe with ends maintained at different temperatures.

Then we introduce the stream function ψ

$$u = \frac{1}{r}\frac{\partial \psi}{\partial \theta}, \quad v = -\frac{\partial \psi}{\partial r}. \tag{9}$$

The governing equations become

$$\nabla^4 \psi = \frac{1}{Pr}\left(\frac{1}{r}\frac{\partial \psi}{\partial \theta}\frac{\partial}{\partial r} - \frac{1}{r}\frac{\partial \psi}{\partial r}\frac{\partial}{\partial \theta}\right)\nabla^2 \psi + Ra\left(\cos\theta \frac{\partial T}{\partial r} - \sin\theta \frac{1}{r}\frac{\partial T}{\partial \theta}\right) \tag{10a}$$

$$\frac{\partial}{\partial r}(\nabla^2 w) = \frac{1}{Pr}\frac{\partial}{\partial r}\left(\frac{1}{r}\frac{\partial \psi}{\partial \theta}\frac{\partial w}{\partial r} - \frac{1}{r}\frac{\partial \psi}{\partial r}\frac{\partial w}{\partial \theta}\right) + Ra \sin\theta \frac{\partial T}{\partial z} \tag{10b}$$

$$\nabla^2 T = \frac{1}{r}\frac{\partial \psi}{\partial \theta}\frac{T}{r} - \frac{1}{r}\frac{\partial \psi}{\partial r}\frac{\partial T}{\partial \theta} + w\frac{\partial T}{\partial z}. \tag{10c}$$

The boundary conditions are equation (6b) and

$$\psi = \frac{\partial \psi}{\partial r} = w = 0 \quad \text{at } r = 1. \tag{11}$$

Now we expand ψ, w, and T into power-series in Ra

$$\psi = \sum_{n=0}^{\infty} \psi_n \left(\frac{Ra}{S}\right)^n \tag{12a}$$

$$w = \sum_{n=0}^{\infty} w_n \left(\frac{Ra}{S}\right)^n \tag{12b}$$

$$T = \sum_{n=0}^{\infty} T_n \left(\frac{Ra}{S}\right)^n \tag{12c}$$

where S is a rescaling parameter which is used to avoid overflow during the computation on the computer. Substituting the expressions (12) into equations (10) and equating terms containing the same power of Rayleigh number, we obtain the following set of equations

$$\nabla^4 \psi_l = \frac{1}{Pr}\sum_{n=0}^{l}\left(\frac{1}{r}\frac{\partial \psi_n}{\partial \theta}\frac{\partial}{\partial r} - \frac{1}{r}\frac{\partial \psi_n}{\partial r}\frac{\partial}{\partial \theta}\right)\nabla^2 \psi_{l-n} + \left(\cos\theta \frac{\partial T_{l-1}}{\partial r} - \sin\theta \frac{1}{r}\frac{\partial T_{l-1}}{\partial \theta}\right)\cdot S \tag{13a}$$

$$\frac{\partial}{\partial r}\nabla^2 w_l = \frac{1}{Pr}\frac{\partial}{\partial r}\sum_{n=0}^{l}\left(\frac{1}{r}\frac{\partial \psi_n}{\partial \theta}\frac{\partial w_{l-n}}{\partial r} - \frac{1}{r}\frac{\partial \psi_n}{\partial r}\frac{\partial w_{l-n}}{\partial \theta}\right) + \sin\theta \frac{\partial T_{l-1}}{\partial z}\cdot S \tag{13b}$$

$$\nabla^2 T_l = \sum_{n=0}^{l}\left(\frac{1}{r}\frac{\partial \psi_n}{\partial \theta}\frac{\partial T_{l-n}}{\partial r} - \frac{1}{r}\frac{\partial \psi_n}{\partial r}\frac{\partial T_{l-n}}{\partial \theta}\right) + \sum_{n=0}^{l} w_n \frac{\partial T_{l-n}}{\partial z}. \tag{13c}$$

The boundary conditions are

$$\psi_l = \frac{\partial \psi_l}{\partial r} = w_l = 0 \quad \text{at } r = 1$$

$$\frac{1}{r^2}\frac{\partial^2 T_l}{\partial \theta^2} + \frac{\partial^2 T_l}{\partial z} = C\frac{\partial T_l}{\partial r} \quad \text{at } r = 1$$

where l is any positive integer. For w_l, we need another boundary condition. From the geometry of the flow, w should be antisymmetrical with respect to the horizontal plane, i.e. $w(r\sin\theta) = -w[r\sin(-\theta)]$, implying $\nabla^2 w = 0$ at $r = 0$. Therefore, we obtain $\nabla^2 w_l = 0$ at $r = 0$ as another boundary condition for w_l. It is easy to show that ψ_l would have non-zero solutions only when l is an even number, and w_l, T_l would have non-zero solutions only when l is an odd number. Then the equation (13) becomes

$$\nabla^4 \psi_{2l} = \frac{1}{Pr}\sum_{n=1}^{l-1}\left(\frac{1}{r}\frac{\partial \psi_{2n}}{\partial \theta}\frac{\partial}{\partial \theta} - \frac{1}{r}\frac{\partial \psi_{2n}}{\partial \theta}\frac{\partial}{\partial \theta}\right)\nabla^2 \psi_{2(l-n)} + \left(\cos\theta \frac{\partial T_{2l-1}}{\partial r} - \sin\theta \frac{1}{r}\frac{\partial T_{2l-1}}{\partial \theta}\right)\cdot S \tag{14a}$$

$$\frac{\partial}{\partial r}\nabla^2 w_{2l-1} = \frac{1}{Pr}\sum_{n=1}^{l-1}\left(\frac{1}{r}\frac{\partial \psi_{2n}}{\partial \theta}\frac{\partial}{\partial r} - \frac{1}{r}\frac{\partial \psi_{2n}}{\partial r}\frac{\partial}{\partial \theta}\right) w_{2(l-n)-1} + \sin\theta \frac{\partial T_{2(l-1)}}{\partial z}\cdot S \tag{14b}$$

$$\nabla^2 T_{2l-1} = \sum_{n=1}^{l-1}\left(\frac{1}{r}\frac{\partial \psi_{2n}}{\partial \theta}\frac{\partial}{\partial r} - \frac{1}{r}\frac{\partial \psi_{2n}}{\partial r}\frac{\partial}{\partial \theta}\right) T_{2(l-n)-1} + w_{2l-1}\frac{\partial T_0}{\partial z}. \tag{14c}$$

It is also easy to show that the zeroth-order solutions are

$$\psi_0 = 0$$
$$w_0 = 0 \tag{14d}$$
$$T_0 = k_1 z + k_2$$

where k_1 and k_2 are undetermined constants which depend on the boundary conditions at the ends of the pipe. In fact, k_1 is the zeroth order temperature gradient $\partial T_0/\partial z$. Later, it will be shown that k_1 strongly depends on the aspect ratio of the pipe and Rayleigh number.

In general, the solutions of the equations (14) are of the following form:

$$\psi_{2l} = k_1^{2l}\sum_{i=1}^{l}\sum_{j=1}^{4l+1} \sin(2i\theta)\cdot r^{2j-2}\cdot E_{2l,i,j} \tag{15a}$$

$$w_{2l-1} = k^{2l-1}\sum_{i=1}^{l}\sum_{j=1}^{4l-2} \sin(2i-1)\theta \times r^{2j-1}\cdot A_{2l-1,i,j} \tag{15b}$$

$$T_{2l-1} = k_1^{2l}\sum_{i=1}^{l}\sum_{j=1}^{4l-1} \sin(2i-1)\theta \times r^{2j-1}\cdot C_{2l-1,i,j} \tag{15c}$$

Then

$$\nabla^4 \psi_{2l} = k_1^{2l}\sum_{i=1}^{l}\sum_{j=1}^{4l-1} \sin(2i\theta) \times r^{2j-2}\cdot G_{2l,i,j} \tag{16a}$$

$$\nabla^4\psi_{2l} = k_1^{2l} \sum_{i=1}^{l} \sum_{j=1}^{4l} \sin(2i\theta) \times r^{2j-2} \cdot F_{2l,i,j} \quad (16b)$$

$$\nabla^2 w_{2l-1} = k_1^{2l-1} \sum_{i=1}^{l} \sum_{j=1}^{4l-3} \sin(2i-1)\theta \times r^{2j-1} B_{2l-1,i,j} \quad (16c)$$

$$\nabla^2 T_{2l-1} = k_1^{2l} \sum_{i=1}^{l} \sum_{j=1}^{4l-2} \sin(2i-1)\theta \times r^{2j-1} D_{2l-1,i,j}. \quad (16d)$$

We use double-precision to compute all the coefficients A, B, C, D, E, F, G from $l = 1$ to $l = 23$ on the IBM 370/3033 machine. Using three-dimensional arrays for these coefficients, we find the computations limited by storage. To overcome this, we map the three-dimensional arrays to one-dimensional arrays to save the two-thirds of each three-dimensional array that is not used during the computing.

The Nusselt number Nu is defined as

$$\frac{Nu}{k_1} = \frac{Q}{\pi r_0 k(T_2^* - T_1^*)k_1} = \frac{1}{\pi k_1}\int_0^{2\pi}\int_0^1 \left(\frac{\partial T}{\partial z} - wT\right) \times r\,dr\,d\theta = 1 - \sum_{l=1}^{23} Nu_l \left(\frac{Rak_1}{S}\right)^{2l} \quad (17)$$

where Q is the heat flux across the pipe.

$$Nu_l = \sum_{n=1}^{l} \sum_{i=1}^{n} \sum_{k=1}^{l-n+1} \sum_{j=1}^{4n-2} \sum_{m=1}^{4(l-n)+3} \times \frac{A_{2n-1,i,j} \cdot C_{2(l-n)+1,k,m}}{2(j+m)} \delta_{i,k}$$

$$\delta_{i,k} = \begin{cases} 0 & i \neq k \\ 1 & i = k \end{cases} \quad (18)$$

The temperature distribution on the pipe wall is

$$T(1, \theta, z)/k_1 = z + \sum_{l=1}^{23} A_l \left(\frac{Rak_1}{S}\right)^{2l-1} \quad (19)$$

where

$$A_l = \sum_{i=1}^{l} \sum_{j=1}^{4l-1} \sin(2i-1)\theta \cdot C_{2l-1,i,j}. \quad (20)$$

The solution (2.15) gives a four-celled flow pattern (see Fig. 2). As the order increases the more cells flow pattern (corresponding to higher order solution) will be added to the basic four-cell flow pattern.

We calculate the coefficients of the Nusselt number series (17) and rewrite (17) as

$$\frac{Nu}{k_1} = \sum_{n=0}^{23} C_n X^n \quad (21)$$

where $X = (Rak_1/S)^2$. The coefficients C_n are shown in Table 1. Note that when $n = 1$, the equation (21) is exactly Bejan and Tien's solution [4]. From now on we shall concentrate on the heat transfer problem and analyze the Nusselt number series.

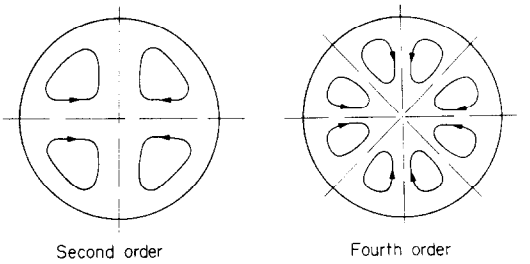

FIG. 2. Pipe cross-section showing streamlines of the second-order and fourth-order flow pattern.

3. EXTENSION OF THE UTILITY OF THE NUSSELT NUMBER SERIES

We have extended Bejan and Tien's two-term solution to 24 terms for Nusselt number. But this series (21) still has limited utility for description of the physical quantity of interest because of its limited radius of convergence. Figure 3 shows that the series diverges when $X > 0.1$. The higher order coefficients, C_n, however, contain a great deal of information about the analytical structure of the solution. We may find the analytical structure of the series by analyzing the singularities of the series.

The signs of the series (21) soon show a repeated pattern of five

$$+ + - - + - + -, \; - + - + +, \; - + - + +, \; - + - + +, - \ldots.$$

This indicates that the series (21) has a conjugate pair of singularities nearest the origin in the complex plane of $X \equiv (Rak_1/S)^2$. Padé approximants to the series (21) and d/dx ln (21) show that this pair of singularities is located at

$$X_c = -0.0795 \pm 0.0634 \cdot i. \quad (22)$$

If we rewrite equation (22) as

$$X_c = R_c e^{\pm i\theta}.$$

Then R_c will be the radius of the convergence of (21), which is

$$R_c = 0.1017 \quad \text{with } \theta = 2.468. \quad (23)$$

Thus the series (21) will diverge when $X > 0.1017$ as indicated by Fig. 3. But this pair of singularities do not have physical meaning; therefore, we may extend the utility of (21) by mapping them away. To do so, we use the following transformation

$$Y = \frac{X}{\sqrt{[(X - X_c)(X - X_c^*)]}}. \quad (24)$$

This maps the singularities to infinity in the Y-plane and maps infinity in the x-plane to a finite point in the

Table 1. Coefficients of Nusselt number series

N	c_n	g_n	f_n	f_{n+1}/f_n
1	1.0000000D 00	1.0000000D 00	1.0000000D 00	
2	1.5190972D 01	1.5443385D 01	2.5898557D 01	2.5898557D 01
3	-1.5301212D 01	1.1911683D 01	5.9398128D 01	2.2934917D 00
4	-3.5833736D 02	1.1814608D 01	1.4861865D 02	2.5020763D 00
5	4.8657932D 03	1.1355467D 01	3.8337272D 02	2.5795734D 00
6	-4.0783066D 04	1.1281950D 01	1.0031135D 03	2.6165491D 00
7	2.3297050D 05	1.1146633D 01	2.6448724D 03	2.6366630D 00
8	-4.8096931D 05	1.1098503D 01	7.0051916D 03	2.6485935D 00
9	-8.7932865D 06	1.1040237D 01	1.8606680D 04	2.6561272D 00
10	1.4786326D 08	1.1007532D 01	4.9514562D 04	2.6611175D 00
11	-1.3468506D 09	1.0974554D 01	1.3193407D 05	2.6645508D 00
12	7.3462274D 09	1.0950583D 01	3.5186637D 05	2.6669865D 00
13	1.2933260D 09	1.0927924D 01	9.3904669D 05	2.6687594D 00
14	-5.8659099D 11	1.0909037D 01	2.5073283D 06	2.6700784D 00
15	8.0791023D 12	1.0891421D 01	6.6972712D 06	2.6710787D 00
16	-6.6413017D 13	1.0875692D 01	1.7894105D 07	2.6718501D 00
17	2.8083924D 14	1.0860964D 01	4.7821181D 07	2.6724545D 00
18	1.4883696D 15	1.0847354D 01	1.2782289D 08	2.6729347D 00
19	-4.4741005D 16	1.0834516D 01	3.4171167D 08	2.6733214D 00
20	5.1723856D 17	1.0822442D 01	9.1361295D 08	2.6736369D 00
21	-3.6539754D 18	1.0810978D 01	2.4429073D 09	2.6738975D 00
22	8.5260432D 18	1.0799988D 01	6.5326156D 09	2.6741152D 00
23	1.9197898D 20	1.0788735D 01	1.7470169D 10	2.6742992D 00
24	-3.5401249D 21	1.0774276D 01	4.6723203D 10	2.6744563D 00

Y-plane. After the transformation the series (21) becomes

$$\frac{Nu}{k_1} = \sum_{n=0}^{23} g_n Y^n \tag{25}$$

where the g_n are new coefficients shown in Table 1. We again form Padé approximants to (25) and d/dy ln (25) to analyze the singularities of (25). We find two singularities on the real axis of the Y-plane, at 1.000 and -1.677. The nearest singularity lies at $Y = 1$, which is consistent with the fixed sign pattern of the coefficient g_n. Therefore, the series (25) has unity radius of convergence, which corresponds to $X \to \infty$ or $Ra \to \infty$. In principle, the series (25) can be used in the case of $Ra \to \infty$. In a practical sense however, the utility of equation (25) is still limited because of its slow convergence when Ra gets large or $Y \to 1$. In order to extend the utility of equation (25), we need to know the nature of the singularity at $Y = 1$. Before we analyze the nature of this singularity, we use an Euler transformation to map away the nonphysical singularity on the negative axis to reduce its influence on (25). The Euler transformation $Z = Y/(Y + 1.677)$ maps the singularity at -1.677 to infinity in the z-plane and maps the singularity at 1 to 0.3736. In the z-plane the series (25) becomes

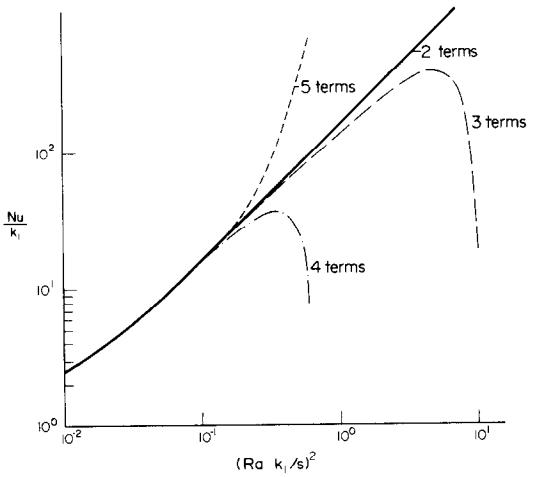

FIG. 3. Nusselt number Nu/k_1 as a function of $(Rak_1/S)^2$ in different order approximation, i.e. second-, third-, fourth- and fifth-order approximation.

$$\frac{Nu}{k_1} = \sum_{n=0}^{23} f_n Z^n \tag{26}$$

where the f_n are new coefficients shown in Table 1. We form Padé approximants to the new series (26) and d/dz ln (26), and find that the nearest singularity is now located at $Z_c = 0.3737$. The Domb–Sykes plot (Fig. 4) and Neville table to Domb–Sykes ratios also suggest that the nearest singularity is located at $Z_c = 0.3736$. In order to analyze the nature of this singularity we suppose

$$\frac{Nu}{k_1} \sim \left(1 - \frac{Z}{Z_c}\right)^{\alpha} \quad \text{as } Z \to Z_c. \tag{27}$$

Then the logarithmic derivative of (27) will become $\alpha/(Z - Z_c)$. Therefore, the residue of the Padé approximants to d/dz ln (26) will give an estimate of the exponent α. This value is about -0.98. On the other hand, from the Ratio method we have the sequences for series (26)

$$fd_n \equiv \frac{f_{n+1}}{f_n} \sim \frac{1}{Z_c}\left[1 - \frac{1+\alpha}{n} + 0\left(\frac{1}{n^2}\right)\right] \tag{28a}$$

$$1 + \alpha = n(n+1)\left(\frac{fd_{n+1}}{fd_n} - 1\right). \tag{28b}$$

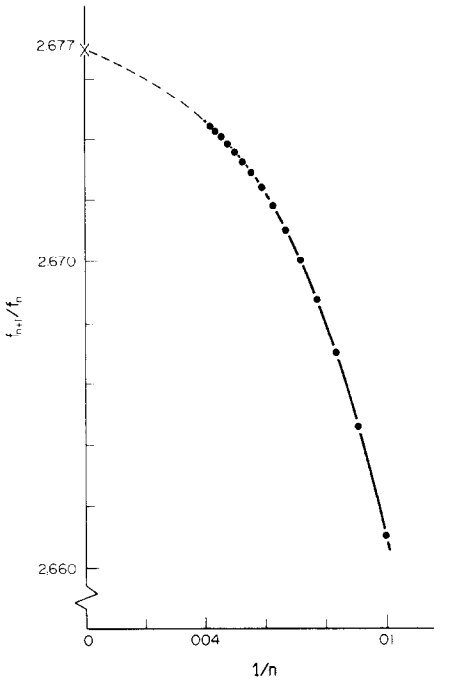

FIG. 4. Domb ratio in the z-plane.

A Neville table for equation 28b gives the estimates of α as -0.986 and -0.987 from quadratic and cubic extrapolations, respectively. Therefore, we may make a mimic function for series (26)

$$\frac{Nu}{k_1} = \left(1 - \frac{Z}{0.3736}\right)^{-1} B(Z) \tag{29}$$

where $B(Z)$ is an extracted series

$$B(Z) = \sum_{n=0}^{23} e_n Z^n. \tag{30}$$

We may use Padé approximants to represent $B(Z)$

$$\begin{aligned} B(Z) = (&1 + 0.145 \times 10^2 Z - 0.108 \times 10^3 Z^2 + 0.174 \times 10^4 Z^3 - 0.159 \times 10^5 Z^4 + 0.669 \times 10^5 Z^5 \\ &- 0.149 \times 10^6 Z^6 + 0.186 \times 10^6 Z^7 - 0.129 \times 10^6 Z^8 + 0.455 \times 10^5 Z^9 - 0.648 \times 10^4 Z^{10} \\ &+ 0.168 \times 10^3 Z^{11})/(1 - 0.880 \times 10^1 Z + 0.105 \times 10^3 Z^2 - 0.772 \times 10^3 Z^3 \\ &+ 0.288 \times 10^4 Z^4 - 0.589 \times 10^4 Z^5 + 0.682 \times 10^4 Z^6 - 0.437 \times 10^4 Z^7 \\ &+ 0.141 \times 10^4 Z^8 - 0.180 \times 10^3 Z^9 + 0.364 \times 10^1 Z^{10}) \end{aligned} \tag{31}$$

4. EFFECT OF THE END BOUNDARY CONDITION ON THE SOLUTION

Notice that we have not considered the boundary conditions in the z-direction so far, and there is an undetermined constant k_1 in the solution for the Nusselt number (17, 29). The value of k_1 depends strongly on the end boundary conditions of the pipe. If we suppose the aspect ratio extremely small $r_0/L \to 0$, then the end boundary condition may be considered as follows:

$$T(r, \theta, 0) \approx 0 \quad T(r, \theta, L/r_0) \approx 1. \tag{32}$$

These determine the values of k_1 and k_2

$$\begin{aligned} k_1 &= r_0/L \\ k_2 &= 0. \end{aligned} \tag{33}$$

Then (29) becomes

$$Nu \cdot \frac{L}{r_0} = \left(1 - \frac{Z}{0.3736}\right)^{-1} \cdot B(Z) \tag{34}$$

where

$$Z = \frac{Y}{Y + 1.677} \tag{35a}$$

$$Y = \frac{X}{\sqrt{[(X - X_c)(X - X_c^*)]}} \tag{35b}$$

$$X = \left[\frac{Ra(r_0/L)}{S}\right]^2. \tag{35c}$$

Equation (34) is an extreme situation when Ra is fixed and r_0/L approaches zero (see Bejan and Tien [4]). But in the real problem, the aspect ratio is fixed and

Rayleigh number is becoming very large. In that case, the end regions of the pipe become very important, and the constants k_1 and k_2 depend very strongly on the Rayleigh number as well as the aspect ratio of the pipe.

In order to estimate the effect of the end condition of the pipe on the heat transfer, we have matched the first-order core solution with an integral solution for the flow and temperature field in the end regions.

We define the end region length δ as that segment of the horizontal enclosure outside which, $Z > \delta$, the core solutions are valid. The integral energy and momentum equations within the end region are

$$\int_0^1\int_0^{2\pi}\left(\frac{\partial T}{\partial z}\right)_{z=0}\mathrm{d}r\,\mathrm{d}\theta = \int_0^1\int_0^{2\pi}\left(\frac{\partial T}{\partial z}\right)_{z=\delta}\mathrm{d}r\,\mathrm{d}\theta + \int_0^1\int_0^{2\pi}\int_0^{\delta}\frac{1}{r}\frac{\partial}{\partial r}\left(r\frac{\partial T}{\partial r}\right)\mathrm{d}r\,\mathrm{d}\theta\,\mathrm{d}z - \int_0^{\delta}\int_0^{2\pi}(uT)_{r=0}\,\mathrm{d}\theta\,\mathrm{d}z - \int_0^1\int_0^{2\pi}(wT)_{z=\delta}\,\mathrm{d}r\,\mathrm{d}\theta - 1 - \int_0^1\int_0^{2\pi}\int_0^{\delta}\frac{uT}{r}\,\mathrm{d}r\,\mathrm{d}\theta\,\mathrm{d}z \tag{36}$$

$$Ra\int_0^1\int_0^{2\pi}\sin\theta\,(T)_{z=\delta}\,\mathrm{d}r\,\mathrm{d}\theta = \int_0^1\int_0^{2\pi}\left(u\frac{\partial u}{\partial r} + \frac{v}{r}\frac{\partial u}{\partial\theta} + w\frac{\partial u}{\partial z} - \frac{v^2}{r}\right)_{z=\delta}\mathrm{d}r\,\mathrm{d}\theta + \int_0^{\delta}\int_0^{2\pi}\left(u\frac{\partial w}{\partial r} + \frac{v}{r}\frac{\partial w}{\partial\theta} + w\frac{\partial w}{\partial z}\right)_{z=0}\mathrm{d}\theta\,\mathrm{d}z + \int_0^{\delta}\int_0^{2\pi}[(\nabla^2 w)_{r=1} - (\nabla^2 w)_{r=0}]\,\mathrm{d}\theta\,\mathrm{d}z - \int_0^1\int_0^{2\pi}[(\nabla^2 u)_{z=\delta} - (\nabla^2 u)_{z=0}]\,\mathrm{d}r\,\mathrm{d}\theta + \int_0^1\int_0^{2\pi}\frac{1}{r^2}(u)_{z=\delta}\,\mathrm{d}r\,\mathrm{d}\theta \tag{37}$$

Then we have to select reasonable profiles for the velocity and temperature distributions inside the end region. We choose the following profiles

$$u = \frac{3Rak_1}{32}\frac{z}{\delta}\left(1-\frac{z}{\delta}\right)(2r - r^2 - 1)\cdot\sin\theta \tag{38a}$$

$$v = \frac{3Rak_1}{32}\frac{z}{\delta}\left(1-\frac{z}{\delta}\right)(r^4 - 4r^2 + 4r - 1)\sin\theta \tag{38b}$$

$$w = \frac{Rak_1}{8}\left(\frac{z}{\delta}\right)^2\left(3 - 2\frac{z}{\delta}\right)\cdot\sin\theta \tag{38c}$$

$$T = (T_{\delta} - \delta k_1)\left[2\frac{z}{\delta} - \left(\frac{z}{\delta}\right)^2\right] + k_1 z \tag{38d}$$

which satisfy the continuity equations (1) and boundary conditions and match the following first-order core solutions

$$(u)_{z=\delta} = 0 \tag{39a}$$

$$(v)_{z=\delta} \tag{39b}$$

$$(w)_{z=\delta} = \frac{Rak_1}{\delta}(r^3 - 1)\sin\theta \tag{39c}$$

$$(T)_{z=\delta} = \frac{Rak_1^2}{192}(r^5 - 3r^3 + 4r)\sin\theta + k_1 z + k_2. \tag{39d}$$

Substituting expressions (38) into the integral equations (36) and (37) yields

$$1.2637\frac{Ra^2k_1^3}{1536} + 6k_1 - \frac{4k_2}{\delta} = 0 \tag{40}$$

$$\delta = 0.87057. \tag{41}$$

We assume the temperature field is symmetric about the center of the pipe, i.e.

$$T\left(0, \theta, \frac{1}{2}\frac{L}{r_0}\right) = \frac{1}{2}$$

which yields

$$k_2 = \frac{1}{2} - \frac{k_1}{2}\frac{L}{r_0}. \tag{42}$$

Combining equations (42) and (40), we obtain

$$ak_1^3 + bk_1 + c = 0 \tag{43}$$

where $a = 8.2269 \times 10^{-4}\,Ra^2$, $b = 6 + 2.2973\,(L/r_0)$, $c = -2.2973$. Obviously, k_1 very strongly depends on the Rayleigh number Ra and the aspect ratio r_0/L. From equation (43), if $r_0/L \to 0$ while Ra is fixed then

$k_1 \to r_0/L$. This is the extreme situation in which the core flow pattern dominates the heat transfer through the pipe. The equation (29) combined with (43) and equation (34) are shown in Fig. 5.

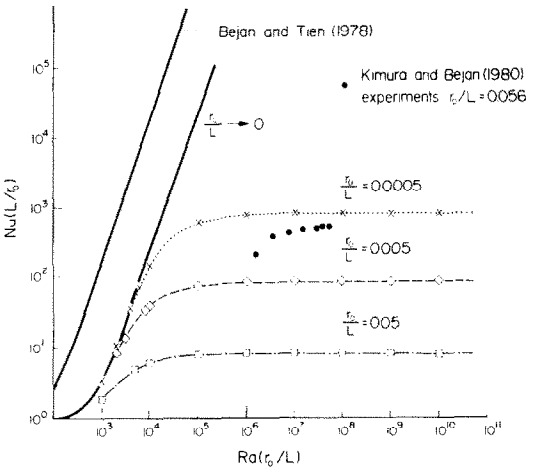

FIG. 5. Nusselt number vs Rayleigh number according to equations (34) and (29) combined with (43).

Finally we should point out that we have assumed fully developed flow in the middle portion of the pipe. This means that r_0/L must be small enough so that our assumption makes sense. Kimura and Bejan's experimental study [6] shows that the core flow is still not fully developed at $r_0/L = 0.056$. We cite their results in Fig. 5.

Acknowledgements—The author thanks Professor Milton Van Dyke of the Mechanical Engineering Department, Stanford University, for helpful advice. The author also thanks Professor I-dee Chang of the Aeronautics and Astronautics Department, Stanford University, and Professor C. L. Tien of the Mechanical Engineering Department, University of California, Berkeley, for many valuable comments.

REFERENCES

1. M. Van Dyke, Analysis and improvement of perturbation series, *Quart. J. Mech. appl. Math.* **27**, 423–450 (1974).
2. M. Van Dyke, Computer extension of perturbation series in fluid mechanics, *SIAM J. appl. Math.* **28**, 720–734 (1975).
3. M. Van Dyke, Extended Stokes series: laminar flow through a loosely coiled pipe, *J. Fluid Mech.* **86**, 129–145 (1978).
4. A. Bejan and C. L. Tien, Fully developed natural conterflow in a long horizontal pipe with different end temperatures, *Int. J. Heat Mass Transfer* **21**, 701–708 (1978).
5. D. S. Gaunt and A. J. Guttmann, Series expansion: analysis of coefficients, pp. 181–243, in *Phase Transitions and Critical Phenomena*, Vol. 3. Academic Press, New York (1974).
6. S. Kimura and A. Bejan, Experimental study of natural convection in a horizontal cylinder with different end temperatures, *Int. J. Heat Mass Transfer* **23**, 1117 (1980).

DEVELOPPEMENT NUMERIQUE DE SERIE: CONVECTION NATURELLE DANS UN TUBE HORIZONTAL AVEC DIFFERENTES TEMPERATURE AUX EXTREMITES

Résumé—Le développement à trois termes de Bejan et Tien est étendu à 47 termes selon le nombre de Rayleigh pour les distributions de vitesse et de température dans la portion médiane d'un tube horizontal avec une paroi adiabatique et des extrémités chauffées différemment. On examine la série pour le nombre de Nusselt et on étend son utilité en analysant ses singularités. On estime aussi l'effet des extrémités en testant la solution du noyau de premier ordre avec une solution intégrale pour l'écoulement et la température dans la région terminale.

DURCH COMPUTER ERWEITERTE REIHENENTWICKLUNG: FREIE KONVEKTION IN EINEM LANGEN HORIZONTALEN ROHR MIT VERSCHIEDENEN ENDTEMPERATUREN

Zusammenfassung—Für die Geschwindigkeits- und die Temperaturprofile in der mittleren Region eines langen horizontalen Rohres mit adiabaten Wänden und unterschiedlich beheizten Enden wurde die dreigliedrige Reihe von Bejan und Tien auf 47 Glieder in der Rayleigh-Zahl erweitert. Die Reihenentwicklung der Nusselt-Zahl wird untersucht und ihre Anwendbarkeit durch Untersuchung ihrer Singularitäten erweitert. Der Einfluß der Enden wird durch Anpassung der Lösung für den Kern, einer Lösung 1. Grades, an die integrale Lösung für Strömungsgeschwindigkeit und Temperatur in den Endgebieten abgeschätzt.

ИССЛЕДОВАНИЕ ЕСТЕСТВЕННОЙ КОНВЕКЦИИ В ДЛИННОЙ ГОРИЗОНТАЛЬНОЙ ТРУБЕ С РАЗНЫМИ ТЕМПЕРАТУРАМИ НА КОНЦАХ С ПОМОЩЬЮ ЭЛЕКТРОННО-ВЫЧИСЛИТЕЛЬНОЙ МАШИНЫ

Аннотация — Для определения профилей скорости и температуры в центральной части длинной горизонтальной трубы с адиабатическими стенками и разными температурами на концах трехчленное разложение, предложенное Беджаном и Тьеном, обобщено на 47 членов по числу Релея. Исследуется разложение в ряд по числу Нуссельта и на основании анализа сингулярностей расширяется область его применимости. Также дана оценка концевых эффектов путем сопоставления решения первого порядка для центральной части с интегральным решением для течения и температуры на концах трубы.